Hindawi Publishing Corporation
Journal of Nanomaterials
Volume 2011, Article ID 691582, 7 pages
doi:10.1155/2011/691582

Research Article

ZnO and MgZnO Nanocrystalline Flexible Films: Optical and Material Properties

Jesse Huso,[1] John L. Morrison,[1] Hui Che,[1] Jency P. Sundararajan,[1] Wei Jiang Yeh,[1] David McIlroy,[1] Thomas J. Williams,[2] and Leah Bergman[1]

[1] *Department of Physics, University of Idaho, Moscow, ID 83844-0903, USA*
[2] *Electron Microscopy Center, University of Idaho, Moscow, ID 83844-0903, USA*

Correspondence should be addressed to Leah Bergman, lbergman@uidaho.edu

Received 14 March 2011; Accepted 25 May 2011

Academic Editor: Xuedong Bai

An emerging material for flexible UV applications is $Mg_xZn_{1-x}O$ which is capable of tunable bandgap and luminescence in the UV range of ~3.4 eV–7.4 eV depending on the composition x. Studies on the optical and material characteristics of ZnO and $Mg_{0.3}Zn_{0.7}O$ nanocrystalline flexible films are presented. The analysis indicates that the ZnO and $Mg_{0.3}Zn_{0.7}O$ have bandgaps of 3.34 eV and 4.02 eV, respectively. The photoluminescence (PL) of the ZnO film was found to exhibit a structural defect-related emission at ~3.316 eV inherent to the nanocrystalline morphology. The PL of the $Mg_{0.3}Zn_{0.7}O$ film exhibits two broad peaks at 3.38 eV and at 3.95 eV that are discussed in terms of the solubility limit of the ZnO-MgO alloy system. Additionally, external deformation of the film did not have a significant impact on its properties as indicated by the Raman LO-mode behavior, making these films attractive for UV flexible applications.

1. Introduction

Flexible electronic structures have been extensively studied due to their distinct advantageous properties such as conforming to irregular surfaces, the ability to sustain bending and deformation, and coating of large areas for ultralight weight applications [1–4]. Flexible devices have potential applications in displays, solar cells, and large-scale sensor arrays. An emerging material that holds promise for flexible applications is ZnO. Due to its deep excitonic energy level, thermal stability, and chemically benign nature, ZnO is increasingly becoming an attractive wide bandgap semiconductor [5]. While there have been a small number of studies on the optical properties of ZnO films grown on flexible substrates, most have used flexible substrates that are transparent in the visible region [6–12]. In those studies, flexible ZnO transistors, light-emitting diodes, and circuits were fabricated, and thin films and nanostructured ZnO were deposited for various optical applications. However, the UV compatibility of a flexible substrate may enhance the potential applications of ZnO-based wide bandgap alloys such as $Mg_xZn_{1-x}O$. This alloy system has been the focus of recent studies due to its bandgap and luminescence tuneability that ranges from the bandgap of ZnO ~3.4 eV to that of MgO ~7.4 eV [13–16]. To our knowledge, to date there are no reports on flexible $Mg_xZn_{1-x}O$ films.

ZnO has the hexagonal wurtzite structure and a deep exciton level ~60 meV, while MgO has the NaCl cubic structure and excitonic binding energy ~140 meV [17, 18]. Due to their deep excitonic binding energies and direct bandgaps, the MgO-ZnO solid solution is an attractive alloy system for the creation of efficient light emissions. However, because of the different crystal structures, the two oxides do not show complete solid solubility. $Mg_xZn_{1-x}O$ thin films over a wide composition range have been grown by pulsed-laser deposition (PLD) and by molecular beam epitaxy (MBE) techniques [13–15, 19–21]. Other research groups have extended research efforts into the field of $Mg_xZn_{1-x}O$ in its nanocrystalline and nanostructure form [16, 22–28]. Key findings are that at Mg composition up to ~30% the alloy is soluble and has mainly the wurtzite structure with tunable bandgap spanning the range of ~3.4 eV–4 eV, while

at the composition range of ~30–60% (referred to as the transition range) the alloy is phase-separated into Zn- and Mg-rich precipitates, and at Mg composition above ~60% it has the cubic structure and bandgaps tuned in the range ~5 eV–7 eV. Recently, a study on ZnO-based films and UV detectors found that by introducing a MgZnO buffer layer of low Mg composition for the epitaxy of MgZnO with high Mg content, a suppression of the phase segregation can be achieved [29]. Our previous studies concerning the optical properties of $Mg_xZn_{1-x}O$ nanocrystals demonstrated that PL renders a useful technique for the investigation of the phase segregation. It was found that at the transition range, the PL of the nanocrystals exhibits multiple emission lines due to the phase segregation of Zn-rich and Mg-rich precipitates in the nanocrystal samples [16].

In this paper, we report on the optical and material properties of ZnO and $Mg_{0.3}Zn_{0.7}O$ grown via a sputtering technique on fluorinated ethylene propylene (FEP) substrate which is flexible and UV transparent. The optical properties of the resulting flexible films were studied via transmission and photoluminescence (PL) spectroscopy, while Raman scattering was utilized to investigate the stress state of the film and the impact of external mechanical deformation. The bandgaps of the ZnO and $Mg_{0.3}Zn_{0.7}O$ films were found to be 3.34 eV and 4.02 eV, respectively. The PL of the ZnO nanocrystalline film was found to exhibit free and bound exciton emissions similar to those of the ZnO bulk material. However, a PL emission about 50 meV below the exciton range was found to be highly pronounced and was attributed to the nanocrystalline morphology of the films. In contrast to the well-defined PL of the ZnO, that of the alloy was found to have broad emission lines in a large energy range, that are discussed in terms of a phase separation phenomenon inherent to the ZnO-MgO solid solution. The Raman analysis indicates that the applied deformation did not have a significant impact on the structural properties of the films, making them promising for potential UV flexible applications.

2. Experiment

The substrate used for the experiments is commercially available FEP, also known as Teflon FEP. The ZnO and the $Mg_{0.3}Zn_{0.7}O$ samples were grown at room temperature on prepared FEP substrates utilizing magnetron sputtering of Zn and Mg-Zn targets, respectively, under argon plasma. The samples were then oxidized for 2 hours under an atmosphere of 99.99% pure oxygen at a temperature of 275°C, which is below the melting temperature of the FEP of ~285°C. The composition of the alloy was determined via energy dispersive spectroscopy (EDS).

The PL and Raman scattering experiments utilized a JY-Horiba micro-Raman/PL system consisting of a high-resolution T-64000 triple monochromator and a UV confocal microscope capable of focusing to a spot size of ~1 μm diameter. A CW-Kimmon laser with a wavelength of 325 nm (3.8 eV) and a Lexel Laser at 244 nm (5.1 eV) were used as the excitation source for the PL, and the cold temperature PL measurements were conducted in an INSTEC UV-compatible microcell. Since the exaction energy used for the Raman scattering (3.8 eV) is close to that of the ZnO bandgap, the LO mode is resonant enhanced which makes it suitable for the analysis of the stress state of the ZnO sample [24, 26, 30]. The experimental error for the Raman frequency is $\pm 1\ cm^{-1}$. The room temperature transmission experiments utilized the Varian-Cary 300 UV-visible system.

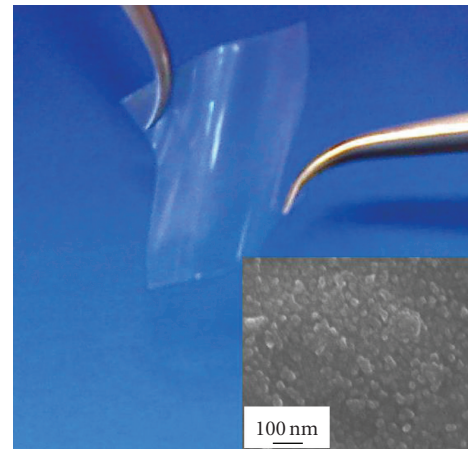

Figure 1: A photograph of the ZnO film and its SEM image (inset) showing a nanocrystalline morphology.

3. Results and Discussion

Figure 1 shows a representative photograph of the resulting ZnO film and the corresponding scanning electron microscopy (SEM) image. The photograph shows that the film is highly flexible, and the SEM image indicates that the ZnO film consists of nanocrystalline morphology. Due to the chemical structure of the FEP, it is unlikely that the ZnO and the $Mg_{0.3}Zn_{0.7}O$ are chemically bonded to the polymer substrate. However, it was observed that even after repeated flexing and deformation, the films remained attached to their respective substrates, suggesting that they become partially embedded in the FEP during the oxidation step so as to create a stable film-substrate system. An SEM image of the $Mg_{0.3}Zn_{0.7}O$ film is presented in Figure 2, and as can be observed in the upper part of Figure 2 (the micron-scale SEM image) the film is highly textured. Previous studies on polytetrafluoroethylene (PTFE), which is a polymer related to FEP, have found that its structure and morphology are sensitive to the choice of cooling rates from the sintering temperature [31, 32]. We leave issue of the surface morphology modification to a future investigation. A representative cross-section SEM image of the $Mg_{0.3}Zn_{0.7}O$ sample is shown in Figure 3, indicating that the thickness of the film is ~3.8 μm; the thickness of the ZnO film was found to be ~5 μm. Atomic force microscopy (AFM) images are additionally presented in Figure 4, and as can be seen in the figure, both films have a granular structure with nonuniform grain size distribution.

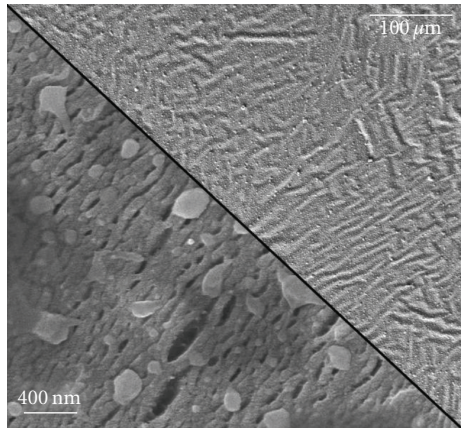

Figure 2: SEM images at two different size-scales of the $Mg_{0.3}Zn_{0.7}O$ flexible film.

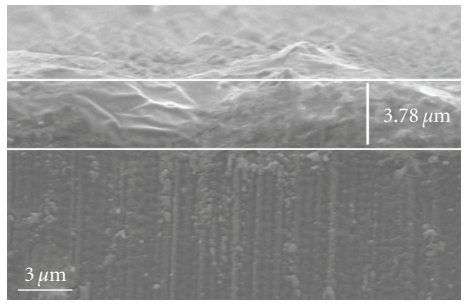

Figure 3: A representative cross-section SEM image of the $Mg_{0.3}Zn_{0.7}O$ film of thickness ~3.8 μm.

In order to identify the crystal structure, X-ray diffraction (XRD) spectra of the ZnO and $Mg_{0.3}Zn_{0.7}O$ films are presented in Figure 5. The diffractions of the ZnO sample are at 31.3° and 36.4°, which register with the reference values of wurtzite ZnO at 31.7° and 36.2°. The XRD peaks of the $Mg_{0.3}Zn_{0.7}O$ films are wide, and we attribute it to the phase segregation in this sample, a finding that is consistent with the absorption and the PL analyses that will be discussed in the next section. The broad background in the XRD is due to the underlying FEP substrate; this background inhibits the identification of the cubic structure phase of the $Mg_{0.3}Zn_{0.7}O$. The average grain size of the ZnO sample was calculated via Scherrer's formula and found to be ~25 nm, a value that is smaller than that obtained from the SEM and AFM images (~60 nm). An observation similar to ours has been reported previously where the grain size of ZnO film calculated from XRD measurements was found to be smaller than that calculated from AFM measurements; these findings were attributed to line broadening mechanisms, other than grain size, such as stress and defects [33]. The wide XRD of the $Mg_{0.3}Zn_{0.7}O$ film prevents a meaningful application of Scherrer's analysis to that sample.

Figure 6 shows the transmission spectra of the ZnO and the $Mg_{0.3}Zn_{0.7}O$ films; the inset to the figure is the transmission spectrum of the bare FEP substrate. The transmission spectrum of the FEP demonstrates its high transparency well into the UV range: at ~5 eV it retains 60% of its transmission, a property which makes it a suitable substrate for the $Mg_xZn_{1-x}O$ alloy system. The bandgaps of the films were determined by computing the derivative transmittance against energy [34]. Our analysis, presented in Figure 7, indicates that the ZnO film has a bandgap of ~3.34 eV at room temperature, which in consistent with previous reports [35], while that of $Mg_{0.3}Zn_{0.7}O$ is at ~4.02 eV, a value similar to that previously observed for a PLD film [13].

The gradual absorption edge of the $Mg_{0.3}Zn_{0.7}O$, as can be seen in Figure 6, may indicate that the alloy is at the phase transition range. To further investigate the solubility of the alloy, PL at room temperature was acquired: Figure 8 depicts the PL spectrum of the $Mg_{0.3}Zn_{0.7}O$ film and that of the ZnO film (see inset). As can be seen in Figure 8, the PL of the alloy film exhibits two broad peaks at 3.38 eV and at 3.95 eV, that can be assigned to PL originating from Zn-rich and Mg-rich distribution of precipitates. Our previous studies of $Mg_xZn_{1-x}O$ nanocrystals, grown via a chemical approach, have found a similar trend in the PL characteristics for crystals at the phase separation range. Specifically, the PL spectra of nanocrystals of Mg composition ~40% were found to have multiple emission lines: the low energy ones corresponding to the Zn-rich of the wurtzite structure, and the higher energy ones corresponding to the Mg-rich [16].

Additionally, as can be seen in the inset to Figure 8, the room-temperature PL of the ZnO film is at 3.26 eV, which is lower than the expected value of the free A-exciton of ZnO [16, 36]. To further investigate this emission, PL at 77 K was acquired: the spectrum of the ZnO film along with that of a reference bulk ZnO crystal are shown in Figure 9. As can be seen in Figure 9, the PL of the bulk ZnO consists of two main emissions at 3.361 eV and at 3.376 eV. These PL emissions have been previously observed and studied by various groups and have been assigned to a neutral donor-bound exciton D^0X and to the free A-exciton (denoted as X), respectively [36]. As is shown in Figure 9, the spectrum of the ZnO film exhibits a PL at 3.370 eV, which is in the same spectral range of the bulk excitons, indicating that the PL is a convolution of the D^0X and the free A-exciton. Additionally, phonon replicas are also present at the lower energy range of the PL spectra of the bulk and the film. A principal finding is that in addition to the excitonic emission line, the PL of the ZnO film exhibits a strong line at 3.316 eV, referred to as the ε-PL, which is redshifted by ~55 meV from the excitonic emission. The ε-emission had been previously reported by us to be the main PL in ZnO nanocrystals of size ~40 nm that were grown via a thermal decomposition method [16]. There it was discussed that the ε-emission is due to surface structural defects. Similar PL emission has also been previously studied in ZnO thin films grown via a PLD method [37]. In particular, optical studies of ZnO thin films utilizing cathodoluminescence (CL) in conjunction with high-resolution imaging techniques have indicated that an emission at ~3.31 eV in the ZnO film originates predominantly from stacking faults, and dangling bonds were suggested to be the possible optical centers [37]. As was mentioned above, the ε-emission was found by us

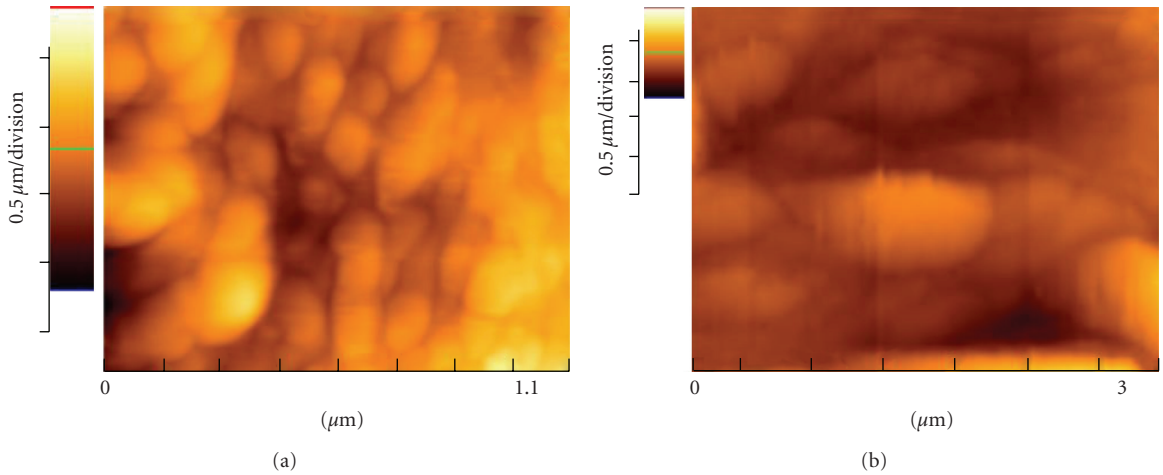

Figure 4: AFM images of the ZnO film (a), and that of $Mg_{0.3}Zn_{0.7}O$ (b).

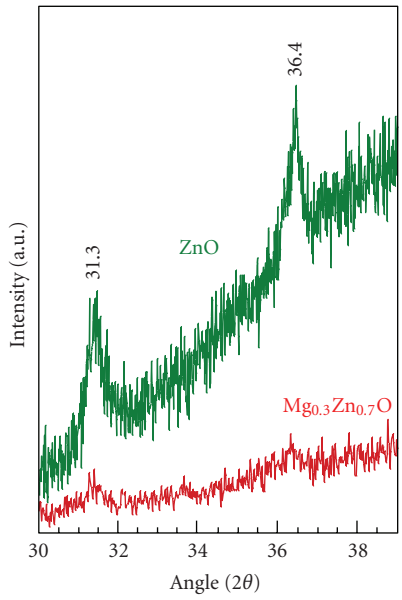

Figure 5: The XRD of the flexible films. The diffraction peaks register with the wurtzite structure.

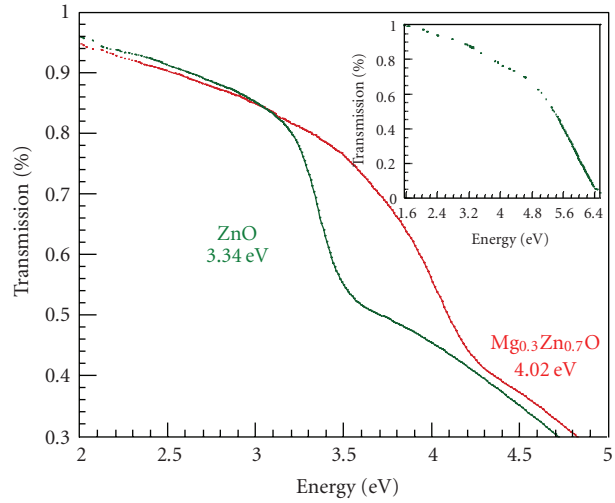

Figure 6: The room-temperature transmission spectra of the ZnO and $Mg_{0.3}Zn_{0.7}O$ films; bandgaps of ~3.34 eV and 4.02 eV, respectively, were obtained. The inset to the figure is the transmission spectrum of the bare FEP substrate indicating a significant UV-transparency.

to be significant also in ZnO nanocrystals that were grown via the thermal decomposition of Zn-acetate. The average size of the crystallites was found to be ~40 nm, and their surfaces were found to exhibit structural surface defects [16]. Additionally, our preliminary results (work to be published elsewhere) on the optical properties of sintered cold-pressed ZnO ceramics of large grain-size ~1 μm and of relatively high-quality surface morphology, have established that the ε-emission is absent in these samples, and the predominant PL is due to D^0X and the free A-exciton as expected. The above points indicate that the ε-emission is a surface-related PL and thus, due to the large surface to volume ratio inherent to the nanocrystalline morphology of the studied samples, this PL emission is expected to be pronounced. Future investigation is merited in order to pinpoint the exact nature and the chemical identity of the ε-emission.

For practical applications, insight into the properties of the films under bending and mechanical deformation can prove useful. To study the effect of flexing, the films were bent at 180° and clamped in a hemostat, and then the resulting highly strained edge was studied via Raman spectroscopy. The results of the experiments are presented in Figures 10(a) and 10(b). In Figure 10(a), the Raman spectra of the LO mode of the ZnO film are presented for both unstrained and strained conditions. Figure 10(b) shows the Raman spectra of the unstrained FEP and that of the ZnO film, as well as the Raman spectrum of the ZnO film under deformation. The spectral range presented in Figure 10(b) is that of the Raman modes of the FEP. It bears noting that FEP is

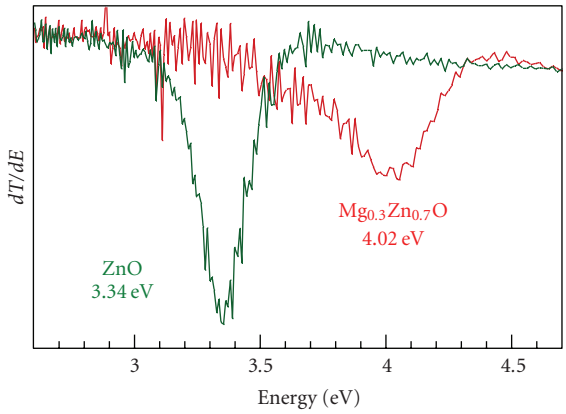

Figure 7: The derivative of the transmission spectra.

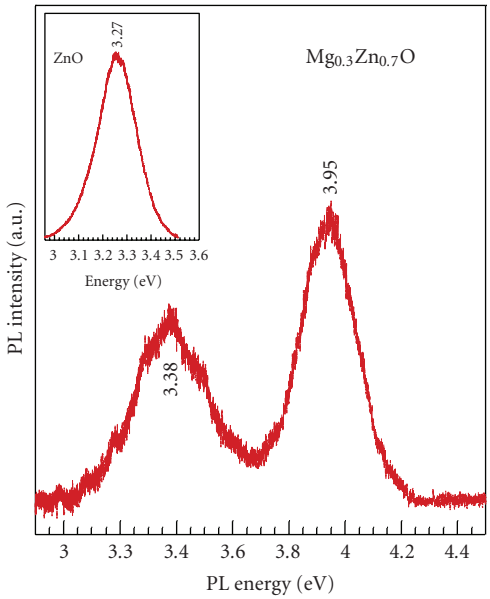

Figure 8: The room-temperature PL of the $Mg_{0.3}Zn_{0.7}O$ film exhibiting two broad emissions at 3.38 eV and 3.95 eV indicative of a phase separation. The inset is the room-temperature PL, at 3.27 eV, of the ZnO film.

a copolymer of tetrafluoroethylene and hexafluoropropylene, and is closely related to the more extensively studied polytetrafluoroethylene (PTFE), also known as Teflon, by the replacement of an F atom with a CF_3 group [38, 39]. The Raman mode frequencies of both materials have been reported in [39, 40] and our results are consistent with theirs, with mode symmetry of A_1 at 1380 cm^{-1}, E_1 at 1299 cm^{-1}, and E_2 at 1217 cm^{-1}.

From the behavior of the Raman modes the following conclusions can be drawn. First, looking at the two lower traces in Figure 10(b) at no deformation condition, the modes of the underlying FEP substrate in the ZnO film exhibit a meaningful redshift frequency up to ~4 cm^{-1} relative to those of the bare FEP, thus implying that in the ZnO film its underlying FEP substrate is under tensile stress.

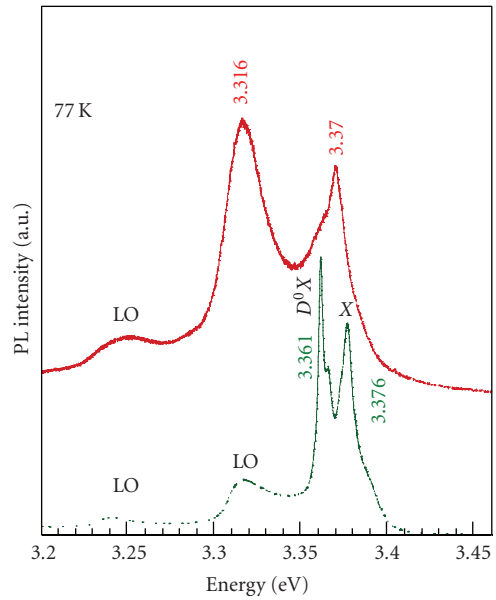

Figure 9: The PL at 77 K of the ZnO film (top) and that of a bulk ZnO crystal (bottom). The bulk ZnO exhibits the bound excitation at 3.361 eV and the free A-exciton at 3.376 eV. The ZnO film exhibits PL in the spectral range of the excitons at ~3.370 eV and in addition a PL at ~3.316 eV attributed to surface defects.

The existence of tensile stress may stem from the very large difference in thermal expansion coefficients between the ZnO at 4.75×10^{-6}/K and that of the transparent substrate, on the order of 10^{-4}/K [41–43]. During the oxidation stage, at a temperature of ~275°C, the FEP substrate was observed to be somewhat malleable. Upon cooling, the large difference in thermal expansion coefficients between the two materials comes into play: due to the ZnO layer the FEP can not contract into its initial state, creating a residual tensile strain in the FEP. The second finding is that the deformation (upper trace in Figure 10(b)) did not impact the underlying FEP substrate, since no frequency shift was observed for the FEP Raman modes. Additionally, there is only a minor impact on the ZnO itself. As can be seen in Figure 10(a), the LO mode of the flexed ZnO sample has a ~2 cm^{-1} redshift relative to that of the unstrained sample, which is somewhat above our experimental error, indicating that the deformation did not result in any significant internal strain in the ZnO layer.

4. Conclusions

In conclusion, ZnO and $Mg_{0.3}Zn_{0.7}O$ nanocrystalline flexible films were achieved utilizing a FEP flexible substrate that is transparent in the portion of the UV range that is compatible to that of the alloys. The analysis indicated that the ZnO film has a room-temperature bandgap of ~3.34 eV, while that of the $Mg_{0.3}Zn_{0.7}O$ film is at ~4.02 eV; thus in that regard bandgap engineered flexible optical alloys were realized. The PL of the ZnO film had emissions due to a neutral donor-bound exciton D^0X and the free A-exciton which are the expected PL from a ZnO bulk material. Additionally, an emission at ~3.316 eV was present whose

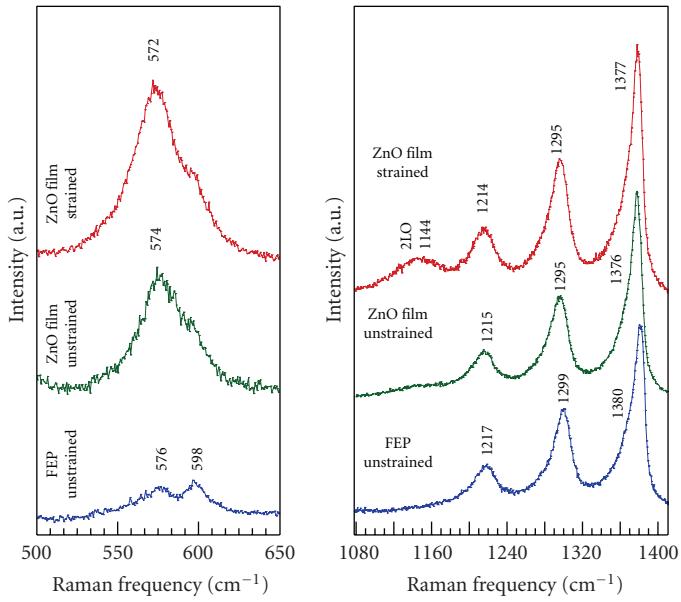

Figure 10: (a) The Raman spectra of the unstrained FEP and the ZnO film (lower two traces) and the spectrum of ZnO film under mechanical deformation (upper trace). The spectra of the ZnO exhibit the LO Raman mode. The deformation resulted in a $\sim 2 \pm 1\ \text{cm}^{-1}$ redshifted frequency, implying that the ZnO itself is under negligible stress. (b) The Raman spectra of the unstrained FEP (lower trace) and that of the ZnO film (middle trace) showing the Raman modes of the FEP. The redshift of the FEP Raman modes indicates that the underlying FEP substrate is under tensile stress. The spectrum of the deformed film (upper trace) implies that the deformation has no impact on the underlying FEP substrate. The 2LO is the second order-mode of ZnO.

origin is discussed in terms of surface-related defects arising from the nanocrystalline morphology of the films. The PL of the $Mg_{0.3}Zn_{0.7}O$ film was found to have two broad peaks at 3.38 eV and at 3.95 eV that were assigned to the Zn-rich and Mg-rich distribution of precipitates, which in turn are due to the inherent limited solubility of the ZnO-MgO solid solution. From the Raman mode behavior it was concluded that in the ZnO film its underlying FEP substrate was under tensile stress. The residual tensile stress was attributed to the large difference of the thermal expansion coefficients of ZnO and that of the FEP. Importantly, the applied external deformation on the ZnO film did not show any effect on its stress state, making these types of films promising for potential UV flexible applications.

Acknowledgments

This research was supported by the U.S. Department of Energy, Office of Basic Energy Science, Division of Materials Science and Engineering under Award DE-FG02-07ER46386. The authors also acknowledge the Center of Materials Characterization at the University of Idaho.

References

[1] W.-Y. Chang, T.-H. Fang, Y. T. Shen, and Y.-C. Lin, "Flexible electronic sensors for tactile multiscanning," *Review of Scientific Instruments*, vol. 80, Article ID 084701, 2009.

[2] T. Sekitani, T. Yokota, U. Zschieschang et al., "Organic nonvolatile memory transistors for flexible sensor arrays," *Science*, vol. 326, no. 5959, pp. 1516–1519, 2009.

[3] Z. Fan, H. Razavi, J. W. Do et al., "Three-dimensional nanopillar-array photovoltaics on low-cost and flexible substrates," *Nature Materials*, vol. 8, no. 8, pp. 648–653, 2009.

[4] P. Heremans, "Semiconductor electronics: organic crystals at large," *Nature*, vol. 444, no. 7121, pp. 828–831, 2006.

[5] Ü. Özgür, Ya. I. Alivov, C. Liu et al., "A comprehensive review of ZnO materials and devices," *Journal of Applied Physics*, vol. 98, no. 4, Article ID 041301, 2005.

[6] E. M. C. Fortunato, P. M. C. Barquinha, A. C. M. B. G. Pimentel et al., "Fully transparent ZnO thin-film transistor produced at room temperature," *Advanced Materials*, vol. 17, no. 5, pp. 590–594, 2005.

[7] K. Nomura, H. Ohta, A. Takagi, T. Kamiya, M. Hirano, and H. Hosono, "Room-temperature fabrication of transparent flexible thin-film transistors using amorphous oxide semiconductors," *Nature*, vol. 432, no. 7016, pp. 488–492, 2004.

[8] D. Zhao, D. A. Mourey, and T. N. Jackson, "Fast flexible plastic substrate ZnO circuits," *IEEE Electron Device Letters*, vol. 31, no. 4, pp. 323–325, 2010.

[9] R. Könenkamp, R. C. Word, and C. Schlegel, "Vertical nanowire light-emitting diode," *Applied Physics Letters*, vol. 85, no. 24, pp. 6004–6006, 2004.

[10] E. S. P. Leong, S. F. Yu, S. P. Lau, and A. P. Abiyasa, "Edge-emitting vertically aligned ZnO nanorods random laser on plastic substrate," *IEEE Photonics Technology Letters*, vol. 19, no. 22, pp. 1792–1794, 2007.

[11] A. N. Banerjee, C. K. Ghosh, K. K. Chattopadhyay et al., "Low-temperature deposition of ZnO thin films on PET and glass substrates by DC-sputtering technique," *Thin Solid Films*, vol. 496, no. 1, pp. 112–116, 2006.

[12] C.-C. Lin, H.-P. Chen, H.-C. Liao, and S.-Y. Chen, "Enhanced luminescent and electrical properties of hydrogen-plasma

ZnO nanorods grown on wafer-scale flexible substrates," *Applied Physics Letters*, vol. 86, no. 18, Article ID 183103, 3 pages, 2005.

[13] A. Ohtomo, M. Kawasaki, T. Koida et al., "$Mg_xZn_{1-x}O$ as a II-VI widegap semiconductor alloy," *Applied Physics Letters*, vol. 72, no. 19, pp. 2466–2468, 1998.

[14] A. K. Sharma, J. Narayan, J. F. Muth et al., "Optical and structural properties of epitaxial $Mg_xZn_{1-x}O$ alloys," *Applied Physics Letters*, vol. 75, no. 21, pp. 3327–3329, 1999.

[15] S. Choopun, R. D. Vispute, W. Yang, R. P. Sharma, T. Venkatesan, and H. Shen, "Realization of band gap above 5.0 eV in metastable cubic-phase $Mg_xZn_{1-x}O$ alloy films," *Applied Physics Letters*, vol. 80, no. 9, pp. 1529–1532, 2002.

[16] J. L. Morrison, J. Huso, H. Hoeck et al., "Optical properties of ZnO and MgZnO nanocrystals below and at the phase separation range," *Journal of Applied Physics*, vol. 104, no. 12, Article ID 123519, 2008.

[17] R. C. Whited, C. J. Flaten, and W. C. Walker, "Exciton thermoreflectance of MgO and CaO," *Solid State Communications*, vol. 13, no. 11, pp. 1903–1905, 1973.

[18] P. D. Johnson, "Some optical properties of MgO in the vacuum ultraviolet," *Physical Review*, vol. 94, no. 4, pp. 845–846, 1954.

[19] T. A. Wassner, B. Laumer, S. Maier et al., "Optical properties and structural characteristics of ZnMgO grown by plasma assisted molecular beam epitaxy," *Journal of Applied Physics*, vol. 105, no. 2, Article ID 023505, 2009.

[20] Z. Vashaei, T. Minegishi, H. Suzuki et al., "Structural variation of cubic and hexagonal $Mg_xZn_{1-x}O$ layers grown on MgO(111)/*c*-sapphire," *Journal of Applied Physics*, vol. 98, no. 5, Article ID 054911, pp. 1–4, 2005.

[21] H. Tampo, H. Shibata, K. Maejima et al., "Strong excitonic transition of $Zn_{1-x}Mg_xO$ alloy," *Applied Physics Letters*, vol. 91, no. 26, Article ID 261907, 2007.

[22] H. -C. Hsu, C. -Y. Wu, H. -M. Cheng, and W. -F. Hsieh, "Band gap engineering and stimulated emission of ZnMgO nanowires," *Applied Physics Letters*, vol. 89, no. 1, Article ID 013101, 2006.

[23] M. Ghosh and A. K. Raychaudhuri, "Structural and optical properties of $Zn_{1-x}Mg_xO$ nanocrystals obtained by low temperature method," *Journal of Applied Physics*, vol. 100, no. 3, Article ID 034315, 2006.

[24] J. Huso, J. L. Morrison, J. Mitchell et al., "Optical transitions and multiphonon Raman scattering of Cu doped ZnO and MgZnO ceramics," *Applied Physics Letters*, vol. 94, no. 6, Article ID 061919, 2009.

[25] K. K. Zhuravlev, W. M. Hlaing Oo, M. D. McCluskey, J. Huso, J. L. Morrison, and L. Bergman, "X-ray diffraction of $Mg_xZn_{1-x}O$ and ZnO nanocrystals under high pressure," *Journal of Applied Physics*, vol. 106, no. 1, Article ID 013511, 2009.

[26] J. Huso, J. L. Morrison, H. Hoeck et al., "Low temperature LO-phonon dynamics of MgZnO nanoalloys," *Applied Physics Letters*, vol. 91, no. 11, Article ID 111906, 2007.

[27] L. Bergman, J. L. Morrison, X. B. Chen, J. Huso, and H. Hoeck, "Ultraviolet photoluminescence and Raman properties of MgZnO nanopowders," *Applied Physics Letters*, vol. 88, no. 2, Article ID 023103, 3 pages, 2006.

[28] H. Matsui, N. Hasuike, H. Harima, and H. Tabata, "Growth evolution of surface nanowires and large anisotropy of conductivity on MgZnO/ZnO quantum wells based on M - nonpolar (10-10) ZnO," *Journal of Applied Physics*, vol. 104, no. 9, Article ID 094309, 2008.

[29] X. Du, Z. Mei, Z. Liu et al., "Controlled growth of high-quality ZnO-based films and fabrication of visible-blind and solar-blind ultra-violet detectors," *Advanced Materials*, vol. 21, no. 45, pp. 4625–4630, 2009.

[30] L. Bergman, X. B. Chen, J. Huso, J. L. Morrison, and H. Hoeck, "Raman scattering of polar modes of ZnO crystallites," *Journal of Applied Physics*, vol. 98, no. 9, Article ID 093507, 4 pages, 2005.

[31] S. M. Wecker, J. B. Cohen, and T. Davidson, "Study of deformation in polytetrafluoroethylene by X-ray line broadening," *Journal of Applied Physics*, vol. 45, no. 10, pp. 4453–4457, 1974.

[32] C. J. Speerschneider and C. H. Li, "Some observations on the structure of polytetrafluoroethylene," *Journal of Applied Physics*, vol. 33, no. 5, pp. 1871–1875, 1962.

[33] B.-Z. Dong, G.-J. Fang, J.-F. Wang, W.-J. Guan, and X.-Z. Zhao, "Effect of thickness on structural, electrical, and optical properties of ZnO: Al films deposited by pulsed laser deposition," *Journal of Applied Physics*, vol. 101, no. 3, Article ID 033713, 2007.

[34] M. Wang, E. J. Kim, S. Kim et al., "Optical and structural properties of sol-gel prepared MgZnO alloy thin films," *Thin Solid Films*, vol. 516, no. 6, pp. 1124–1129, 2008.

[35] V. Srikant and D. R. Clarke, "On the optical band gap of zinc oxide," *Journal of Applied Physics*, vol. 83, no. 10, pp. 5447–5451, 1998.

[36] B. K. Meyer, H. Alves, D. M. Hofmann et al., "Bound exciton and donor-acceptor pair recombinations in ZnO," *Physica Status Solidi (B)*, vol. 241, no. 2, pp. 231–260, 2004.

[37] M. Schirra, R. Schneider, A. Reiser et al., "Stacking fault related 3.31-eV luminescence at 130-meV acceptors in zinc oxide," *Physical Review B*, vol. 77, no. 12, Article ID 125215, 2008.

[38] J. M. Crosby, C. A. Carreno, and K. L. Talley, "Melt processible fluoropolymer composites," *Polymer Composites*, vol. 3, no. 2, pp. 97–100, 1982.

[39] M. J. Hannon, F. J. Boerio, and J. L. Koenig, "Vibrational analysis of polytetrafluoroethylene," *The Journal of Chemical Physics*, vol. 50, no. 7, pp. 2829–2836, 1969.

[40] J. F. Rabolt and B. Fanconi, "Raman scattering from finite polytetrafluoroethylene chains and a highly oriented TFE-HFP copolymer monofilament," *Macromolecules*, vol. 11, no. 4, pp. 740–745, 1978.

[41] Y. Araki, "Thermal expansion coefficient of polytetrafluoroethylene in the vicinity of its glass transition at about 400∘K," *Journal of Applied Polymer Science*, vol. 9, no. 2, pp. 421–427, 1965.

[42] H. Ibach, "Thermal expansion of silicon and zinc oxide (II)," *Physica Status Solidi (B)*, vol. 33, no. 1, pp. 257–265, 1969.

[43] R. D. Vispute, V. Talyansky, S. Choopun et al., "Heteroepitaxy of ZnO on GaN and its implications for fabrication of hybrid optoelectronic devices," *Applied Physics Letters*, vol. 73, no. 3, pp. 348–350, 1998.